A NOVEL TECHNIQUE FOR MULTI USER MULTIPLE ACCESS SPATIAL MODULATION USING ADAPTIVE CODING AND MODULATION

Urvashi Tembhare[1], Kamal Niwaria[2]
1(M.Tech Scholar Electronics and Communication Department, RKDF Institute of Sciences &Technology, and SRK University, Bhopal
Email: tembhareurvi0611@gmail.com)
2 (Asst. Professor Electronics and Communication Department, RKDF Institute of Sciences &Technology, and SRK University, Bhopal
Email: kamalniwaria@gmail.com)

Abstract

The need for high peak data rates with the corresponding need for significantly increased spectral efficiencies, and the support for service specific quality of service (QoS) requirements are the key elements that drive the research in the area of wireless communication access technologies Since space constellations and signal constellations are orthogonal, the well-known digital signal modulation schemes can be used on top. The spatial multiplexing gain comes from the simultaneous transmission of spatially encoded bits. Analytical and numerical performance of SM in different channel conditions, including practical channel considerations, are studied and compared to existing MIMO techniques in this thesis. Results show that SM achieves low BER (bit error ratio) with a tremendous reduction in receiver complexity without sacrificing spectral efficiency.

Key words- MIMO, Spatial Modulation, BER, Bit Error Rate, Modulation Technique etc.

I. INTRODUCTION

The upsurge of wireless communication systems such as vehicle-to-vehicle (V2V) communication [1] and wireless high definition (HD) television have fuelled research into MIMO technology. In recent years, MIMO has been considered as one of the core techniques for improving data throughput, link reliability and spectral efficiency [2-4]. MIMO techniques can be divided into two main categories, namely spatial diversity and spatial multiplexing schemes. Spatial diversity techniques [5, 6] improve link reliability by transmitting multiple redundant copies of data to a receiver over independent channels. Alamouti's scheme [6] is a popular transmit diversity technique, which uses a pair of transmit antennas to achieve full transmit diversity. However, diversity gains are traded off by low spectral efficiency, which remains unchanged when compared to a single-input multiple-output (SIMO) system [7].

Among the set of existing technologies, multiple-input multiple-output (MIMO) with adaptive coding and modulation is promising candidate for future wireless systems. MIMO system boosts the spectral efficiency by using multiple transmit-antennas to simultaneously transmit data to the receiver. Adaptive modulation and coding enables robust and spectrally-efficient transmission over time-varying channels. The basic premise is to estimate the channel at the receiver and feed this estimate back to the transmitter, so that the transmission scheme can be adapted relative to the channel characteristics. The idea is to consider the transmit antenna array as a spatial constellation diagram with the constellation points being the actual antennas. Each spatial constellation point is then mapped to a different bit sequence. At any time instant, only one antenna transmits energy, and the actual information resides in the actual physical location of the transmitting antenna, or spatial constellation point. This, of course, requires a new detection process at the receiver, namely the antenna detection.

IV. RELATED WORK

Space shift keying (SSK) modulation in [28] can be considered as a special instance of SM, since only the transmit antenna indices carry information. The SSK scheme eliminated the use of conventional modulation techniques, which reduced receiver complexity as compared to SM. Furthermore, this decrease in receiver complexity was attained without sacrificing performance gains. Similar to SM, SSK schemes work only for a number of transmit antennas which are a power of two. In cases where the transmit antenna constraint cannot be met, the generalized SSK (GSSK) scheme [29] provides a viable solution. In [29], GSSK used a combination of antenna indices to transmit information, which may be

applied to any antenna configuration. However, the flexibility of GSSK is traded off by reduced performance as compared to SSK [29].

Fractional bit encoded spatial modulation (FBE-SM) in [30], which is a more versatile SM scheme based on the theory of modulus conversion. The FBE-SM approach allowed the transmitter to function with an arbitrary number of antennas. As a result, this scheme is well suited to compact mobile devices, where space constraints pose limits on the number of transmit antennas. Numerical results have shown that FBE-SM offers flexibility in design and the necessary degrees of freedom for trading-off attainable performance and capacity [30].

Trellis coded spatial modulation (TCSM) in [31], which applied trellis coded modulation (TCM) to the antenna constellation points of SM. This increased the free distance between antenna constellation points, thus leading to improved performance over spatially correlated channels. The TCSM scheme was analyses in [32], where an analytical framework for the performance over correlated fading channels was proposed.

Soft-output ML detection in [33], where a soft-output ML detector for SM orthogonal frequency division multiplexing (OFDM) systems was introduced and shown to outperform the conventional hard decision based SM detector.

SM with partial channel state information (CSI) at the receiver in [34], where an SM detector with unknown phase reference at the receiver was developed and analyzed. Monte Carlo simulations were used as a tool to verify the analytical frameworks and investigate the performance of the proposed detector. Results indicated that SM performance was severely degraded when phase information was not available at the receiver. This highlights the fact that accurate channel estimation is required for the efficient operation of SM detectors [34].

Optical spatial modulation (OSM) in [35], which is an indoor optical wireless communication technique based on SM. The OSM scheme was shown to achieve twice and four times the data rate as compared to conventional on-off keying and pulse-position modulation techniques, respectively [35]. In [36], channel coding was applied to OSM and the BER performance of both hard and soft detectors were determined analytically. Monte Carlo simulation results demonstrated that the application of channel coding techniques can enhance OSM performance by approximately 5dB and 7dB for hard and soft decisions, respectively [36].

Normalized maximum ratio combining (NMRC) detector in [37], where a low complexity sub-optimal SM detection algorithm for unconstrained channels was proposed. In addition, an antenna index (AI) list based detector was also introduced in [37]. Monte Carlo simulation results and corresponding analysis indicated that the AI list based scheme can achieve near optimal performance and reduced complexity when compared to the optimal SM detector. However, the AI list based detector can only operate efficiently for list sizes equal to half the number of transmit antennas. This resulted in a 40% increase in complexity as compared to the NMRC scheme.

Space-time block coded spatial modulation (STBC-SM) in [38], which combined SM and STBC in order to exploit the transmit diversity potential of MIMO channels. The proposed scheme was analyzed in [38], where a closed form expression for the average BER was derived. Monte Carlo simulations results were used to support analytical frameworks and also demonstrated the performance advantages of STBC-SM over SM. Results indicated that STBC-SM offers performance enhancements of 3dB-5dB (depending on the spectral efficiency) over conventional SM [38]. It must be highlighted that a similar scheme termed Alamouti coded spatial modulation is proposed in this dissertation. However, both schemes have been developed independently based on the different paradigms employed.

SM–MIMO

In this section, we commence by introducing the SM– MIMO concept, illustrating it with the aid of some simple examples. Again, we denote by Nt and Nr the number of TAs and RAs, respectively. The cardinality of the signal constellation diagram is denoted by M. Either PSK or QAM are considered. In general, Nt, Nr, andM can be chosen independently of each other. At the receiver, optimum ML demodulation is considered. Thus, Nr can be chosen independently of Nt . For ease of exposition, we assume $N_t = 2^{n_t}$ and $M = 2^m$with nt and m being two positive integers. In Section IV, we describe general SM–MIMO encodings as well as some suboptimal (non-ML) demodulation schemes.

In Fig. 1, the SM–MIMO concept is illustrated for Nt = M = 2, and it is compared to the conventional SMX scheme and the OSTBC scheme designed for transmit diversity. In the latter case, the Alamouti scheme is considered as an example [80].

In SMX–MIMO, two PSK/QAM symbols (S1 and S2) are simultaneously transmitted from a pair of TAs in a single channel use. For arbitrary Nt and M, the rate of SMX is $R_{SMX} = N_t log_2(M)$bpcu.

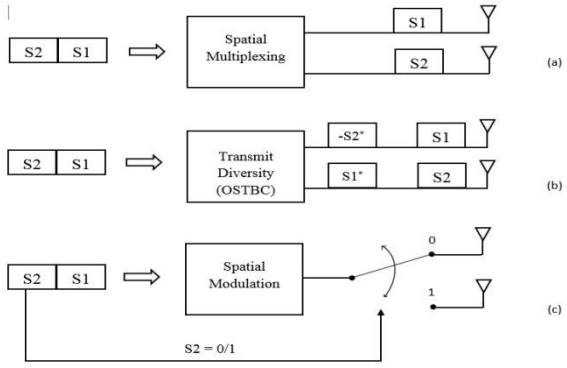

Figure 1 Illustration of three MIMO concepts: (a) spatial multiplexing; (b) transmit diversity; and (c) SM.

In OSTBC–MIMO, two PSK/QAM symbols (S1 and S2) are first encoded and then simultaneously transmitted from a pair of TAs in two channel uses. For arbitrary Nt and M, the rate of OSTBC is $R_{OSTBC} = R_c log_2(M)$bpcu, where $R_c = N_M/N_{cu} \leq 1$ is the rate of the space-time block code and NM is the number of information symbols transmitted in Ncu channel uses If, as shown in Fig. 1, the Alamouti code is chosen, then we have Rc = 1.

In SM–MIMO, only one (S1) out of the two symbols is explicitly transmitted, while the other symbol (S2) is implicitly transmitted by determining the index of the active TA in each channel use. In other words, in SM–MIMO, the information symbols are modulated onto two information carrying units: a) one PSK/QAM symbol; and b) a single active TA via an information-driven antenna-switching mechanism. For arbitrary Nt and M, the rate of SM is$R_{SM} = log_2(M) + log_2(N_t)$ bpcu [76], [82].

In Figs. 2 and 3, the encoding mechanism of SM–MIMO is illustrated for Nt = M= 4 by considering two generic channel uses, where the concept of ‘‘SM or spatialconstellation diagram’’ is also introduced. The rate of this MIMO setup is $R_{SM} = log_2(M) + log_2(N_t) = 4$ bpcu, hence the encoder processes the information bits in blocks of four bits each. In the first channel use shown in Fig. 2, the block of bits to be encoded is ‘‘1100.’’ The first $log_2(N_t) = 2$bits, ‘‘11,’’ determine the single active TA (TX3), while the second$log_2(M) = 2$ bits, ‘‘00,’’ determine the transmitted PSK/QAM symbol. Likewise, in the second channel use shown in Fig. 3, the block of bits to be encoded is ‘‘0001.’’ The first $log_2(N_t) = 2$ bits, ‘‘00,’’ determine the single active TA (TX0), while the second $log_2(M) = 2$ bits, ‘‘01,’’ determine the transmitted PSK/QAM symbol.

The activated TA may change every channel use according to the input information bits. Thus, TA switching is an effective way of mapping the information bits to TA indices and of increasing the transmission rate. It is worth mentioning here that the idea of increasing the rate of wireless communications using TA switching has been alluded in pioneering MIMO papers under the concept of ‘‘spatial cycling using one transmitter at a time’’.

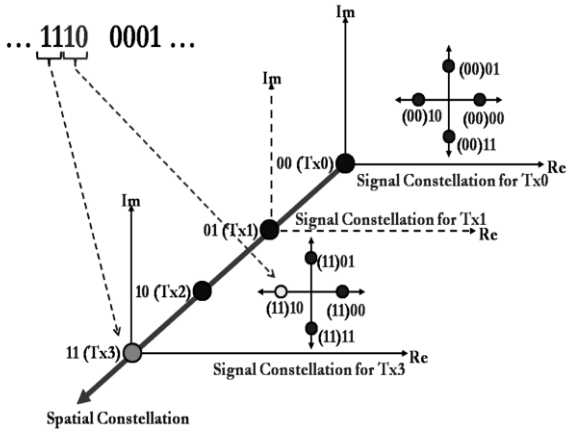

Figure 2 Illustration of the 3-D encoding of SM (first channel use).

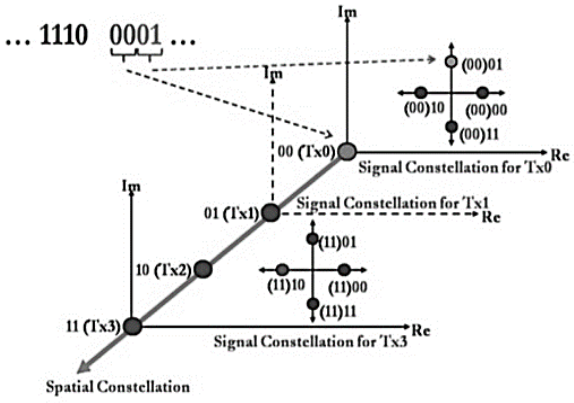

Figure 3 Illustration of the 3-D encoding of SM (second channel use).

The information bits are modulated onto a 3-D constellation diagram, which generalizes the known 2-D (complex) signal-constellation diagram of PSK/QAM

modulation schemes. The thirddimension is provided by the antenna array, where some of the bits are mapped to the TAs. In SM–MIMO research, this third dimension is termed the ‘‘spatial-constellation diagram’’ [76]. In simple mathematical terms, the signal model of SM– MIMO, assuming a frequency-flat channel model, is as follows:

$$\mathbf{y} = \mathbf{Hx} + \mathbf{n}$$

where $\mathbf{y} \in \mathbb{C}^{N_r \times 1}$ is the complex received vector; $\mathbf{H} \in \mathbb{C}^{N_r \times N_t}$ is the complex channel matrix; $\mathbf{n} \in \mathbb{C}^{N_r \times 1}$is the complex AWGN at the receiver; and $\mathbf{x} = \mathbf{e}s \in \mathbb{C}^{N_t \times 1}$ is the complex modulated vector with $s \in \mathcal{M} \subseteq \mathbb{C}^{1 \times 1}$ being the complex (scalar) PSK/QAM modulated symbol belonging to the signal-constellation diagram and $\mathbf{e} \in \mathcal{A}$ being the Nt×1 vector belonging to the spatial-constellation diagram$\mathcal{A}$ as follows:

$$\mathbf{e}_t = \begin{cases} 1, \text{if the } t\text{th TA is active} \\ 0, \text{if the } t\text{th TA is not active} \end{cases}$$

where e_t is the t^{th} entry of e for t = 1, 2,...,N_t. In other words, the points (N_t-dimensional vectors) of the spatialconstellation diagram are the Nt unit vectors of the natural basis of the N_t-dimensional Euclidean space.

If N_t = 1, SM–MIMO reduces to conventional singleantenna communications, where the information bits are encoded only onto the signal-constellation diagram. In this case, the rate is$R_0 = log_2(M)$. On the other hand, if M = 1 the information is encoded only onto the spatial-constellationdiagrambyproviding $e_t$equalto$R_{SSK} = log_2(N_t)$. In particular, SSK modulation is a MIMO scheme, where data transmission takes place only through the informationdriven TA switching mechanism. It is apparent that SM– MIMO can be viewed as the combination of single-antenna PSK/QAM and SSK–MIMO modulations.

II. PROPOSED METHODOLOGY

The system model of the proposed 2 user MA-SM with AMC is shown in Fig. 4, which consists of a MIMO wireless link. We have two user transmitters, transmitting over a Rayleigh fading channel to a common receiver. The receiver is a SM demodulator with a ML detector explained in previous section. The receiver calculates the joint probability of the two received signals. The ML detector then computes the Euclidean distance between the received vector signal and the set of all possible received signals, selecting the closest one.

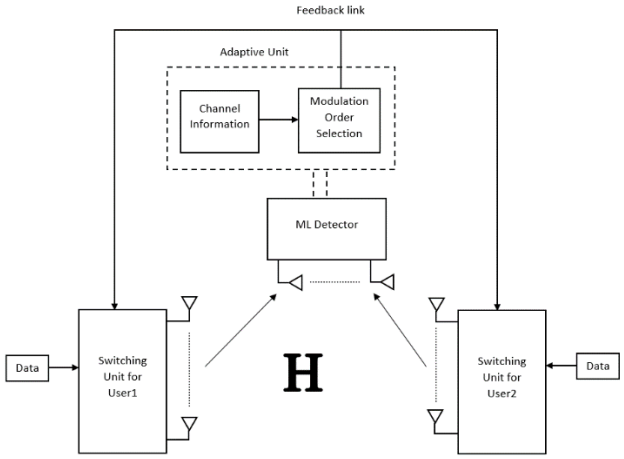

Figure 4. 2-user Multiple Access Spatial Modulation with ACM System Model

At the user end, in contrast to conventional SM which uses the same modulation order for data mapping, in the proposed scheme, the modulation orders assigned to transmit antennas are chosen by the switching unit. More specifically, when the channel is slowly varying, the adaptive unit at the receiver computes the optimum candidate for transmission and sends this information to the two users through a low-bandwidth feedback path. The transmitters then employ the corresponding modulation orders for the next channel use.

The Adaptive unit uses the channel state information obtained by the receiver to decide the optimum level of modulation. It then relays it back to the transmitters of the two users, which utilize this information to modulate the next transmitted signal accordingly. If the nature of the channel changes, then so does the modulation order. This is done by predefining a minimum and maximum level of BER. The receiver then compares the BER of the received signal to the pre-set values, for a signal that has a lower BER value than desired, the frame size of the transmitted signal can be increased and for a signal that has higher BER value than desired, the frame size of the transmitted signal is reduced. Quintessentially, we aim to optimally use the channel bandwidth available to us. According to the requirement and characteristics of the channel, the transmitter adapts itself to the best modulation scheme so as to maintain BER for better spectral efficiency.

V. RESULTS AND SIMULATION

In this section, we study and compare the graphs obtained for various levels of channel attenuation with and without ACM.

Each simulation graph shown below consists of four results. The pink and cyan graphs depict the results for two user multiple access spatial modulation without ACM. The red and blue graphs denote the outcomes of our proposed methodology with ACM. As can be seen in the following section, we consider the different variations in the simulation results by varying the channel attenuation of the system. This change in channel attenuation leads to change in the CSI and shows adaptive modulation in action. The graphs study the BER of the system in reference to the SNR in dB of the proposed scheme. The main aim as stated is to minimize BER of the received signal, and by merely studying the graph it is beautifully apparent. Also, if we do a detailed deliberation of each case and compare the results with previous outcomes, we can easily see and analyze the changes in the various outcomes for different inputs.

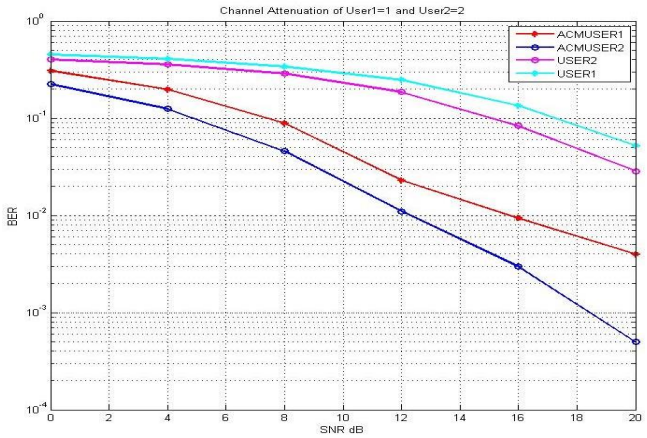

Figure 5 Comparison Results for users 1 and 2 with and without ACM and channel attenuation of 1 and 2 dB respectively.

This graph illustrates the behavior of the signal with and without ACM for channel attenuation of User1 and User2 as 1 and 2 respectively. For the graph without ACM i.e. only multiple access spatial modulation the BER is higher. It does gradually decrease with the SNR but doesn't go lower than 0.001 whereas in the presence of ACM, the BER is more of a straight line and sharply decreases to the lower bound values. The upper and lower bound values of BER are predefined so as to maintain it in a prescribed range and modulate accordingly.

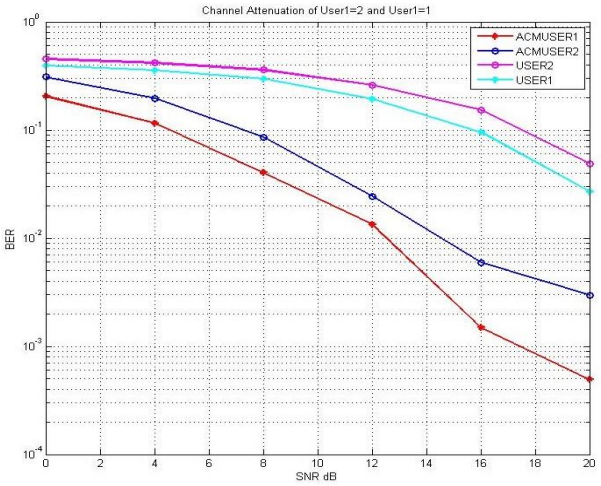

Figure 6 Comparison Results for users 1 and 2 with and without ACM and channel attenuation of 2 and 1 dB respectively.

Now, this graph is a reversal of the previous one. Here the values are similar except the fact that the channel attenuation for user1 is now 2 and for user2 is 1. The behaviour is identical as was in the previous graph. This is because we are working in a system that calculates joint probability of both the received signals and thus the result always remains the same. The behavior is predominantly dependant on the channel properties. This stems the fact that irrespective of the number or position of the TA, the behaviour of the receiver remains the same.

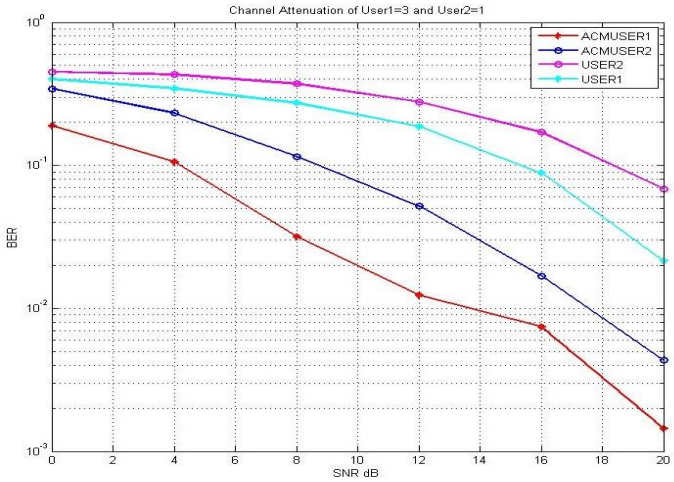

Figure 7 Comparison Results for users 1 and 2 with and without ACM and channel attenuation of 3 and 1 dB respectively.

In this graph, we increase the channel attenuation of user1 to 3 while maintaining channel attenuation of user2 at 1. The behavior of user2 shows the BER is higher and for user1 the BER is lower but more sharply decreasing. If we compare it to the previous graph, where user2 was still

1 the graph is steeper and by increasing the channel attenuation of user1, the receiver properties change to lowering the overall value of BER.

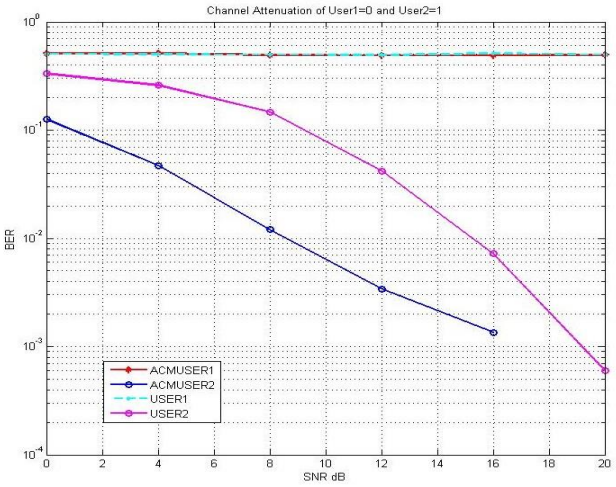

Figure 8 Comparison Results for users 1 and 2 with and without ACM and channel attenuation of 0 and 1 dB respectively.

For a more in depth study, the channel attenuation of user1 is further lowered to 0 and that of user2 is still 1. The result now is vastly different as can be seen. For user1 transmission with and without ACM the BER of both is at a constant value. This might be because the receiver can no longer calculate the minimum distance and thus no variation in the BER. Whereas for the case of user2, with ACM the graph abruptly cuts off. This needs to be studied in more depth to understand the behaviour of the systems.

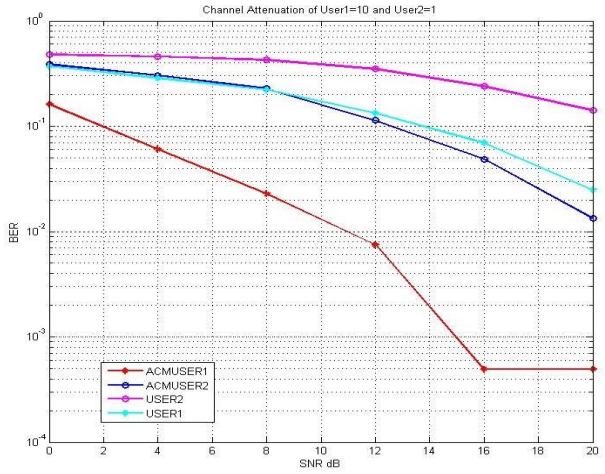

Figure 9 Comparison Results for users 1 and 2 with and without ACM and channel attenuation of 10 and 1 dB respectively.

Let us up the ante now by taking channel attenuation of user 1 as 10. When the difference in channel attenuation value is high the receiver sends back information to compensate for the BER and thus the BER of the other user, user2 in this case drastically increases. The BER of user1 is lower than in any of the previous cases.

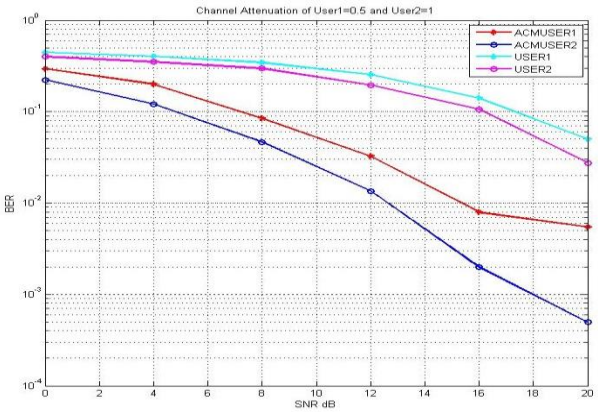

Figure 10 Comparison Results for users 1 and 2 with and without ACM and channel attenuation of 0.5 and 1 dB respectively.

This is an interesting graph. As we can see the channel attenuation of user1 is 0.5 here i.e. between 0 and 1. The graph shows properties closer to the case of channel attenuation being 1. This leads to the conclusion that if the difference in channel attenuation is small then the difference in the BER values also reduces. Although the behaviour remains the same.

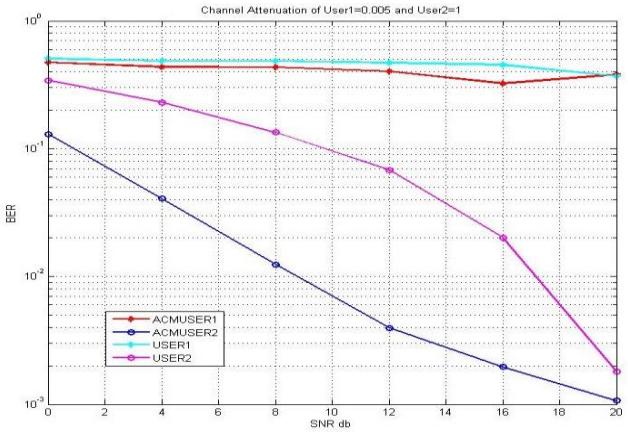

Figure 11 Comparison Results for users 1 and 2 with and without ACM and channel attenuation of 0.005 and 1 dB respectively.

Further decreasing the channel attenuation of user1 to 0.005 shows an entirely new result, which is somewhere in between the BER values of users with channel attenuation of 0 and 1. Both user1's with and without ACM, are nearly at a constant value as it was for the case of channel attenuation 0. But the second users, just show a more extended declining version the graph. It can be assumed that the receiver is trying to balance the two

channel attenuation values for an efficient use of the channel, which is actually what we set out to achieve.

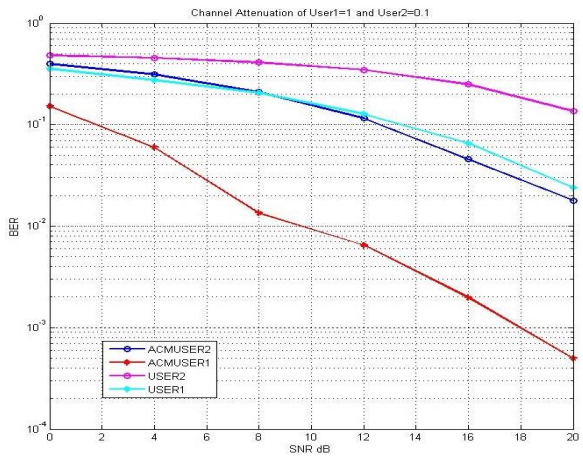

Figure 12 Comparison Results for users 1 and 2 with and without ACM and channel attenuation of 1 and 0.1 dB respectively.

For channel attenuation values of 1 and 0.1 for user1 and user2 respectively. The graph for multiple access SM case is not much different just a little lower than it was before. This leads to the user with ACM to overlap with it for the case of 0.1 channel attenuation.

III. CONCLUSION

The performance of 2 user multiple access spatial modulation with adaptive coding and modulation was studied. The ML receiver was successfully implemented in the Rayleigh fading channel and used to enhance the performance through ACM. For different channel attenuation values and changing number of antennas the impact on BER was studied. The BER shows a significant improvement with ACM as opposed to without ACM. We also studied the BER of the two users for various changes in the channel attenuation. The receiver shows consistent performance characteristics for both users, which was also a point of concern. As we utilized the concept of joint probability to optimize both of the obtained signals.

The generalization of this system for multiple user with different modulation techniques can be studied in the future. Applying coding schemes to this multiple user interface should impact BER and can be further investigated.In recent years, many solutions have been proposed independently with the aim of simplifying the design of MIMO communications. We believe that this trend reinforces the potential impact of SM–MIMO research in the context of next-generation wireless systems.

References:

[1] L. Lu, G. Y. Li, A. L. Swindlehurst, A. Ashikhmin, and R. Zhang, “An overview of massive MIMO: Benefits and challenges,” IEEE J. Sel. Areas Commun., vol. 8, no. 5, pp. 742–758, Oct. 2014.

[2] J. G. Andrews, S. Buzzi, W. Choi, S. V. Hanly, A. Lozano, A. C. K. Soong, and J. C. Zhang, “What will 5G be?” IEEE J. Sel. Areas Commun., vol. 32, no. 6, pp. 1065–1082, Jun. 2014.

[3] V. W. Wong, R. Schober, D. W. K. Ng, and L.-C. Wang, Key technologies for 5G wireless systems. Cambridge university press, 2017.

[4] E. Dahlman, G. Mildh, S. Parkvall, J. Peisa, J. Sachs, Y. Seln, and J. Skld, “5G wireless access: Requirements and realization,” IEEE Commun. Mag., vol. 52, no. 12, pp. 42–47, Dec. 2014.

[5] R. Mesleh, H. Haas, C. W. Ahn, and S. Yun, “Spatial modulation - a new low complexity spectral efficiency enhancing technique,” in Proc. IEEE Int. Conf. Commun. Netw. in China, Beijing, China, Oct. 2006, pp. 1–5.

[6] R. Y. Mesleh, H. Haas, S. Sinanovic, C. W. Ahn, and S. Yun, “Spatial modulation,” IEEE Trans. Veh. Technol., vol. 57, no. 4, pp. 2228–2241, Jul. 2018.

[7] M. D. Renzo, H. Haas, A. Ghrayeb, S. Sugiura, and L. Hanzo, “Spa- tial modulation for generalized MIMO: Challenges, opportunities, and implementation,” Proc. IEEE, vol. 102, no. 1, pp. 56–103, Jan. 2014.

[8] M. Di Renzo, H. Haas, and P. M. Grant, “Spatial modulation for multiple- antenna wireless systems: A survey,” IEEE Commun. Mag., vol. 49, no. 12, pp. 182–191, Dec. 2021.

[9] P. Yang, M. Di Renzo, Y. Xiao, S. Li, and L. Hanzo, “Design guidelines for spatial modulation,” IEEE Commun. Surveys Tuts., vol. 17, no. 1, pp. 6–26, First quarter 2015.

[10] P. Yang, Y. Xiao, Y. L. Guan, K. V. S. Hari, A. Chockalingam,S. Sugiura, H. Haas, M. Di Renzo, C. Masouros, Z. Liu, L. Xiao,S. Li, and L. Hanzo, “Single-carrier SM-MIMO: A promising design for broadband large-scale antenna systems,” IEEE Commun. Surveys Tuts., vol. 18, no. 3, pp. 1687–1716, Third quarter 2016.

[11] A. Stavridis, S. Sinanovic, M. Di Renzo, and H. Haas, “Energy evalua- tion of spatial modulation at a multi-antenna base station,” in Proc. IEEE Veh. Technol. Conf. (VTC Fall), Las Vegas, NV, USA, Sept. 2013, pp. 1–5.

[12] A. Stavridis, S. Sinanovic, M. Di Renzo, H. Haas, and P. Grant, “An energy saving base station employing spatial modulation,” in Proc. IEEE Int. Workshop on Comput. Aided Modeling and Design of Commun. Links and Netw. (CAMAD), Barcelona, Spain, Sept. 2012, pp. 231–235.

[13] D. A. Basnayaka, M. Di Renzo, and H. Haas, “Massive but few active MIMO,” IEEE Trans. Veh. Technol., vol. 65, no. 9, pp. 6861–6877, Sept. 2016.

[14] Y. Cui and X. Fang, “Performance analysis of massive spatial modulation MIMO in high-speed railway,” IEEE Trans. Veh. Technol., vol. 65, no. 11, pp. 8925–8932, Nov. 2016.

[15] J. Jeganathan, A. Ghrayeb, L. Szczecinski, and A. Ceron, "Space shift keying modulation for MIMO channels," IEEE Trans. Wireless Commun., vol. 8, no. 7, pp. 3692–3703, Jul. 2019.
[16] M. D. Renzo, D. D. Leonardis, F. Graziosi, and H. Haas, "Space shift keying (SSK) MIMO with practical channel estimates," IEEE Trans. Commun., vol. 60, no. 4, pp. 998–1012, Apr. 2019.
[17] J. Choi, "Sparse signal detection for space shift keying using the Monte Carlo EM algorithm," IEEE Signal Process. Lett., vol. 23, no. 7, pp. 974–978, Jul. 2016.
[18] H. W. Liang, W. H. Chung, and S. Y. Kuo, "Coding-aided K-means clustering blind transceiver for space shift keying MIMO systems," IEEE Trans. Wireless Commun., vol. 15, no. 1, pp. 103–115, Jan. 2016.
[19] M. Di Renzo and H. Haas, "Improving the performance of space shift keying (SSK) modulation via opportunistic power allocation," IEEE Commun. Lett., vol. 14, no. 6, pp. 500–502, Jun. 2018.
[20] ——, "Bit error probability of space-shift keying MIMO over multiple- access independent fading channels," IEEE Trans. Veh. Technol., vol. 60, no. 8, pp. 3694–3711, Oct. 2018.
[21] ——, "Space shift keying (SSK) modulation with partial channel state information: Optimal detector and performance analysis over fading channels," IEEE Trans. Commun., vol. 58, no. 11, pp. 3196–3210, Nov. 2019.
[22] A. Younis, N. Serafimovski, R. Mesleh, and H. Haas, "Generalised spatial modulation," in Proc. Conf. Rec. 44th Asilomar Conf. Signals, Syst. Comput, Pacific Grove, CA, USA, Nov. 2019, pp. 1498–1502.
[23] J. Fu, C. Hou, W. Xiang, L. Yan, and Y. Hou, "Generalised spatial mod- ulation with multiple active transmit antennas," in Proc. IEEE Globecom Workshops (GC Wkshps), Miami, FL, USA,Dec. 2019, pp. 839–844.
[24] J. Wang, S. Jia, and J. Song, "Generalised spatial modulation system with multiple active transmit antennas and low complexity detection scheme," IEEE Trans. Wireless Commun., vol. 11, no. 4, pp. 1605–1615, Apr. 2018.
[25] B. Zheng, X. Wang, M. Wen, and F. Chen, "Soft demodulation algo- rithms for generalized spatial modulation using deterministic sequentialmonte carlo," IEEE Trans. Wireless Commun., vol. 16, no. 6, pp. 3953– 3967, Jun. 2017.
[26] R. Mesleh, S. S. Ikki, and H. M. Aggoune, "Quadrature spatial modu- lation," IEEE Trans. Veh. Technol., vol. 64, no. 6, pp. 2738–2742, Jun. 2015.
[27] Y. Bian, X. Cheng, M. Wen, L. Yang, H. V. Poor, and B. Jiao, "Differential spatial modulation," IEEE Trans. Veh. Technol., vol. 64, no. 7, pp. 3262–3268, Jul. 2015.
[28] N. Ishikawa and S. Sugiura, "Unified differential spatial modulation,"
IEEE Wireless Commun. Lett., vol. 3, no. 4, pp. 337–340, Aug. 2014.
[29] M. Wen, X. Cheng, Y. Bian, and H. V. Poor, "A low-complexity near- ML differential spatial modulation detector," IEEE Signal Process. Lett., vol. 22, no. 11, pp. 1834–1838, Nov. 2015.
[30] L. Yang, "Transmitter preprocessing aided spatial modulation for multiple-input multiple-output systems," in Proc. IEEE Veh. Technol. Conf. (VTC Spring), Yokohama, Japan, May 2021, pp. 1–5.
[31] A. Stavridis, S. Sinanovic, M. Di Renzo, and H. Haas, "Transmit precod- ing for receive spatial modulation using imperfect channel knowledge," in Proc. IEEE Veh. Technol. Conf. (VTC Spring), Yokohama, Japan, May 2021, pp. 1–5.
[32] R. Zhang, L. Yang, and L. Hanzo, "Generalised pre-coding aided spatial modulation," IEEE Transactions on Wireless Communications, vol. 12, no. 11, pp. 5434–5443, Nov. 2018.
[33] ——, "Error probability and capacity analysis of generalised pre-coding aided spatial modulation," IEEE Transactions on Wireless Communica- tions, vol. 14, no. 1, pp. 364–375, Jan. 2015.
[34] J. Jeganathan, A. Ghrayeb, and L. Szczecinski, "Generalized space shift keying modulation for MIMO channels," in Proc. IEEE Int. Symp. Personal, Indoor, Mobile Radio Commun. (PIMRC), Cannes, France, Sept. 2018, pp. 1–5.
[35] E. Basar, M. Wen, R. Mesleh, M. D. Renzo, Y. Xiao, and H. Haas, "Index modulation techniques for next-generation wireless networks," IEEE Access, vol. 5, pp. 16 693–16 746, 2017.
[36] B. Zheng, M. Wen, F. Chen, N. Huang, F. Ji, and H. Yu, "The K-best sphere decoding for soft detection of generalized spatial modulation," IEEE Trans. Commun., vol. 65, no. 11, pp. 4803–4816, Nov. 2017.
[37] P. Yang, Y. Xiao, Y. Yu, and S. Li, "Adaptive spatial modulation for wireless MIMO transmission systems," IEEE Commun. Lett., vol. 15, no. 6, pp. 602–604, Jun. 20119.
[38] P. Yang, Y. Xiao, L. Li, Q. Tang, Y. Yu, and S. Li, "Link adaptation for spatial modulation with limited feedback," IEEE Trans. Veh. Technol., vol. 61, no. 8, pp. 3808–3813, Oct. 2020